AAPS PharmSciTech (2023) 24:93
https://doi.org/10.1208/s12249-023-02540-9

RESEARCH ARTICLE

The Effect of Design and Size of the Fluid-Bed Equipment on the Particle Size-Dependent Trend of Particle Coating Thickness and Drug Prolonged-Release Profile

Teja Brezovar[1,2] · Grega Hudovornik[2] · Matjaž Perpar[3] · Matevž Luštrik[1,4] · Rok Dreu[1]

Received: 23 December 2022 / Accepted: 23 February 2023 / Published online: 1 April 2023

Abstract
The focus of the current work is to study and demonstrate the impact of the design, the scale, and settings of fluid-bed coating equipment on the differences in pellet coating thickness, which in case of prolonged-release pellets dictates the drug release. In the first set of coating experiments, the pellet cores were coated with the Tartrazine dye with the aim of estimating the coating equipment performance in terms of coating thickness distribution, assessed through color hue. In the second set, drug-layered pellets were film-coated with prolonged-release coating and dissolution profile tests were performed to estimate the thickness and uniformity of the coating thickness among differently sized pellets. In both study parts, film coating was performed at the laboratory and the pilot scale and essentially two types of distribution plate and different height adjustments of the draft tube were compared. The dye coating study proved to be extremely useful, as the results enable process correction and the optimal use of the process equipment in combination with the appropriate process parameters. Preferential film coating of larger drug-containing pellets was confirmed on the laboratory scale, while on the pilot scale, it was possible to achieve preferential coating of smaller pellets using rational alternatives of settings, which is desirable in terms of particle size-independent drug release profile of such prolonged-release dosage forms.

Keywords pellet film coating · Wurster chamber · swirl generator · prolonged release · preferential coating

Introduction

The production of pellets is a widely used process in the pharmaceutical industry, as pellets in a form of multiple-unit systems bring many advantages over single-unit dosage forms (e.g., less risk of "dose dumping" and less local GIT burden), and are therefore often used as a coating substrate for the production of prolonged-release dosage forms [1–4]. Pellets are not the final pharmaceutical form, as they are filled into a capsule or compressed into a tablet [5]. The most common methods of producing pellets in the pharmaceutical industry are still extrusion and spheronization, followed by drug layering, where in the first stage, the active ingredient is sprayed onto the neutral cores. This is usually followed by film coating, which ensures protection of the active ingredient from environmental influences or modified drug release (gastro-resistant, prolonged-release pellets). Pellet coating process can be performed with liquid (solution/suspension) or with powder components in case of dry powder layering [3]. When coating pellets, one must take into consideration their size distribution. The particle size distribution influences pellet properties, such as pellet mass to cross-sectional ratio, which can in turn be the drive for particles to receive different coating amount.

Most known pellet coating device in the industry is classical Wurster chamber (CW), which, when first introduced into production led to improved quality of the coating process, as its configuration ensured repeatable and controlled movement of particles, which was significantly more robust when compared to coating in drums [3]. The characteristic movement of particles in CW ensures the formation of a

✉ Rok Dreu
rok.dreu@ffa.uni-lj.si

1 Faculty of Pharmacy, University of Ljubljana, Aškerčeva cesta 7, 1000, Ljubljana, Slovenia

2 Krka, d.d., Novo mesto, Šmarješka cesta 6, 8501 Novo mesto, Slovenia

3 Faculty of Mechanical Engineering, University of Ljubljana, Aškerčeva cesta 6, 1000 Ljubljana, Slovenia

4 Faculty of Medicine, University of Ljubljana, Vrazov trg 2, 1000 Ljubljana, Slovenia

high-quality coating with good adhesion, as the coating and drying phases alternate. The spray nozzle is inserted from below, slightly above the plate level in the centerline of the draft tube, which allows the coating liquid to be sprayed in the direction fluidizing air flow, while assuring short distance between sprayed droplets and upwards moving particles [6–9]. Wurster-based fluid bed is not a standard fluid bed since the particles exhibit a circular motion in the chamber. It is therefore better described as a circular fluid-bed process with a characteristic slightly pulsating spouted bed. Four distinct regions within the process equipment chamber can be identified, where different types of particle transport take place. First is the up-bed region inside the draft tube, where particles are accelerated by high air velocity and where the coating mass transfer takes place. In the deceleration region, the particles enter the expansion part of the coating chamber where they are dried and diminish velocity due to the fact that superficial air velocity drops below the particle terminal velocity. Next is the down-bed region, where particles are again gaining momentum due to gravity and low local superficial air velocity causing particles to fall onto particle bed formed at the bottom of coating chamber. The openings of the distribution plate below the Wurster draft tube create radially oriented draft, creating a horizontal transport region, which feeds particles inside the partition and completes the circular movement process [9].

It is however known that the thickness of the coating applied in CW depends on the particle size. According to the conclusions of existing studies, larger particles receive more coating and consequently have different properties (e.g., active ingredient content) [6, 10, 13, 14]. There are several reasons for the differences in the amount of coating received, and they all contribute to different time distribution between two consecutive passes through the coating zone and the amount of coating that a particle receives during one pass which has predominant impact [11, 15, 16]. Due to the smaller ratio between the cross section and the mass, smaller particles accelerate faster and, as a result, pass the spraying area inside the draf tube in shorter time, and after exiting the cylinder, they fly higher and therefore circulate through the cylinder less often (longer circulation time). A larger ratio of mass to projected area for larger particles causes shadowing of the smaller particles in the coating zone which also contributes to larger coating gain of the larger particles [11, 14, 18].

Marucci and his colleagues showed that more pellets with a thinner prolonged-release coating mean faster drug release, and they found that the reason for the unevenness of the coating is in the dropout of particles from the coating process due to particles adhering to the observation window as a result of the electrostatic charge buildup [13]. The occurrence of an unevenly thick coating is already noticeable when using particles of a comparable sizes [11, 19], but it is even more pronounced in the case of wider particle size distribution [6, 10, 13, 14], which is often used in real, industrial systems. With the need for functional coating of smaller and smaller particles and at the same time increasingly strict requirements for the quality of the final product, there is a need to upgrade classic Wurster draft tube-based coating systems. With the aim of changing the dynamics of particle movement and consequently ensuring a more uniform thickness of the coating, regardless of the properties of the input material, modifications of CW design in a form of swirl flow generators were introduced (SW). The first version was a conically shaped swirl flow generator with the narrowing part of the cross section at the nozzle [12, 20]. This ensures that the distribution of particles in the cylinder is more random, the particles are more separated from each other, and their speed is higher [20]. For the second version of the swirl generator, the generator with oblique grooves arranged radially with respect to the nozzle was introduced. Luštrik and co-workers showed that the particles move in a swirl-like manner away from the nozzle tip and along the cylinder wall [18], which also results in a higher coating efficiency than with the CW [14, 19]. On the laboratory scale, it has been independently shown several times that the use of eddy current in different coater versions significantly reduces the relative standard deviation (RSD) of the coating thickness among pellets [14, 19, 20].

In addition to the geometrical properties of the coating chamber, the evenness of the applied coating among particles can also be significantly influenced by the process parameters, namely the flow rate of fluidization air, the height of the gap between the distribution plate and the draft tube, pellets loading (the mass of the pellets that are coated), and the atomization air pressure [16, 19]. According to Mann renewal theory, interparticle coating thickness variability reduces, if interparticle shadowing is reduced in the coating zone [11] if circulation time variability is low and number of coating cycles increases [15]. The latter depends on total coating time, particle mass flow rate through the coating zone, and particle loading in the coater [15, 16].

Presented coating study consists of two parts. In the first part, the objective was to determine the influence of the fluid-bed geometrical configuration and equipment size on the phenomena of preferential coating dependent on differently sized starting pellets by using Tartrazine dye as a coating gain marker. The gap between distribution plate and draft tube and type of distribution plate was also varied. In the second part of the study, the same equipment was used while altering critical process variables to evaluate the robustness of the film-coating process in case of prolonged drug release pellet formulation.

Materials and Methods

Materials

In the first part of the study, neutral MCC pellets (Cellets 700, IPC Process Center GmbH, Germany) were coated with water solution composed of 8% w/w HPMC 6 mPas (Shin-Etsu Chemical, Japan), 1% w/w Macrogol 6000 (Clariant Produkte GmbH, Glendorf site, Germany), 1% w/w coloring agent Tartrazine (Sigma-Aldrich, USA), and purified water (90%, w/w).

In the second part of coating experiments, API-coated pellets containing Diclofenac sodium were coated with water-based sustained release coating dispersion containing Eudragit RS 30D (9.6% w/w), Eudragit RL 30 D (19.2% w/w) (Evonic Nutrition Care GmbH, Germany), 1.7% w/w triethyl citrate (Vertellus LLC, USA), and 10.4% w/w talc.

Methods

Pellet Film-Coating Experiments with Tartrazin

Coating experiments using Tartrazine dye were performed on two laboratory-sized fluid-bed coaters (GPCG1, Glatt GmbH, Germany and BX FBD10, Brinox d.o.o., Slovenia) and on one pilot-sized (BX FBD30, Brinox d.o.o., Slovenia) fluid-bed coater. In case of both laboratory coaters, the type of distribution plate and the gap between the plate and the draft tube were varied. The pilot-scale setup with three swirl generators and draft tubes was used, while only the size of the gap was varied during coating experiments (Table I). All other process parameters were comparable within each coating process scale.

Pilot-scale experiments were conducted using three spraying nozzles (0.8 mm) at spraying pressure of 4.2 bar and dispersion flow rate of 50 g/min, while lab-scale experiments were conducted using single nozzle (0.8 mm) at spraying pressure of 1.8 bar and dispersion flow rate 9.9 g/min (exp. T1–T4) or at spraying pressure of 2.5 bar and dispersion flow rate of 14 g/min (exp. T5–T8). All parameters were set to achieve product temperature of 40 ± 2°C. The coating process was finished when predefined mass of suspension was sprayed, and drying phase was performed in the period until the product temperature reached 45°C at lab scale and 50°C at pilot scale. All Tartrazin coating experiments exhibited agglomerate percentage of less than 2% (w/w).

Prolonged-Release (PR) Film-Coating Experiments

API-coated pellets were film coated with prolonged-release formulation using two different sizes of fluid-bed equipment (pilot-scale BX FBD30 and laboratory-scale BX FBD10). Within experiments on both coating equipment scales, the gap between distribution plate and draft tube was varied; on laboratory scale, the type of distribution plate (classical plate *vs.* swirl flow plate subtypes) was also changed.

Table I List of All Preformed Coating Experiments with Coloring Agent Tartrazin (T Designated Experiments) and with Prolonged-Release Formulation (P Designated Experiments)

Experiment	Distribution plate	The gap	Equipment used	Experiment scale
T1	CW	10 mm	GCPG1	1 kg
T2	CW	20 mm	GCPG1	1 kg
T3	SW_B	10 mm	GCPG1	1 kg
T4	SW_B	20 mm	GCPG1	1 kg
T5	CW	25 mm	BX FBD10	3 kg
T6	CW	15 mm	BX FBD10	3 kg
T7	SW_A	25 mm	BX FBD10	3 kg
T8	SW_A	15 mm	BX FBD10	3 kg
T9	SW_A	10 mm	BX FBD30	15 kg
T10	SW_A	20 mm	BX FBD30	15 kg
PR1	SW_A	20 mm	BX FBD30	10 kg
PR2	SW_A	10 mm	BX FBD30	10 kg
PR3	CW	25 mm	BX FBD10	4 kg
PR4	SW_A	25 mm	BX FBD10	4 kg
PR5	SW_A	15 mm	BX FBD10	4 kg

Two subtypes of distribution plate with swirl generator were used: flat (A) and funnel shaped (B)

The coating suspension was prepared in a 30% excess at room temperature. For 4-kg laboratory experiment, 2407.6 g of coating dispersion was prepared in order to spray 1852 g of coating dispersion with theoretical weight gain of 9.6%. 1.000 kg of water was weighed into a 2-L stainless steel container, and 0.250 kg of Pharma talc was mixed into it using pitched baled impeller at 650 rpm. The resulting suspension was homogenized for 10 min with an UltraTurrax mixer set at 8000 rpm. In another 5-L container, we first mixed 0.231 kg of Eudragit RS (30% polymer dispersion) and 0.462 kg of Eudragit RL 30D (30% polymer dispersion), which were previously filtered through a sieve with openings of 0.50 mm. Of talc suspension, 1.250 kg was added with stirring at 650 rpm, and the residue in the vessel was washed with 0.423 kg of water, and finally, 41.6 g of triethyl citrate was added with stirring. The suspension was stirred at 400 rpm for another half an hour. For 10-kg pilot-scale coating experiment, 15,000 g of coating dispersion was prepared in a 50-L stainless steel duplicator equipped with bottom installed propeller impeller operated at 500 rpm. All material amounts were proportionally higher. Analogously, talc suspension was homogenized using Ultra-Turrax in a 5-L beaker. Pilot-scale film-coating experiments were conducted

using three spraying nozzles (inner diameter of 1.2 mm) using spraying pressure of 2.2 bar, while in lab-scale experiments, we used 1 nozzle (1.2 mm) and spraying pressure of 2.0 bar. All parameters were set to achieve bulk product temperature 30 ± 2°C. Coating process was finished when predefined mass of suspension was sprayed, and then drying phase was performed till product temperature reached 35°C.

Coating dispersion amount was defined in the preliminary reference experiment, by taking samples with different coating gains and subsequently analyzing the drug dissolution. We identified coating mass which assured ≥ 60% of the drug released in 6 h. Target theoretical weight gain was 8.0%, assuming the 83% coating yield.

After coating, pellets were placed on a tray and additional 24-h curing step was performed in laboratory-sized convection oven drying chamber to achieve constant drug release profiles. The airflow was constant (30 m^3/h). Air was drawn from the room with normal lab conditions which resulted in curing conditions of about 20% RH at 40°C. All prolonged-release coating experiments exhibited agglomerate percentage equal or close to zero.

List of all experiments with variables is presented in Table I.

Evaluation of Coating Thickness and Pellet Size

Pellet size and coating thickness were optically determined using two-step approach [21]. In the first step, picture of pellets was taken using computer optical scanner (model Epson Perfection V700 Photo, Epson, Japan) with the image capturing resolution set at 1200 dpi. In the second step, images were analyzed for maximum ferret diameter (F_{max}) and perpendicular to maximum ferret diameter (F_{90}) by using in-house image analysis program (based on open-source machine vision library open cv 3.0).

In order to determine applied coating thickness for Tartrazine dye experiments, the key parameter (besides the pellet size) was color hue (h median), since the use of a transparent coating with the addition of a dye meant that the intensity of the pellets color hue increased as the thickness of the coating increased. After pellets were segmented from image background by using Canny edge detection algorithm, color of pixels within pellet boundary was analyzed and transformed to hue-saturation-value color space. The median hue value of all recorded pixels within individual pellet boundary was identified and used in further analysis.

Spectrophotometric calibration curve was prepared for each individual sets of experiments on laboratory and pilot scale, by using Tartrazin 0.067 M K_2HPO (pH 6.5) solutions with different concentrations and measuring their absorbance at 425 nm.

Two coating calibration experiments, where we took pellet samples at predefined time intervals, were carried out. For each time sample, we measured pellet size ($a = F_{max}$ / 2, $b = F_{90}$ / 2) and color hue. To calculate coating thickness of samples from calibration experiments also pellet sample surface was determined for each time point (S_{sample}) using semi-axis a and b and Knud Thomsen approximative equation for surface area of single prolate particle S_1 [22]

$$S_1 = 4\pi\left(\frac{2(ab)^{1.6075} + b^{2\times1.6075}}{3}\right)^{\frac{1}{1.6075}}$$

The exact same pellet sample was measured for absorbance at 425 nm after dissolving the coating in phosphate buffer. The Tartrazine mass was calculated using a spectrophotometric calibration line. The density of the coating was evaluated separately by preparing film samples in a pan and then assessing sample apparent density *via* helium pycnometry. The overall volume of the coating for each pellet sample was calculated from data of calibration sample coating mass and coating density. Coating thickness was then determined by using the following approximation equation valid for small coating thickness

$$t = V_{coating}/S_{sample}$$

where $V_{coating}$ represents sample coating volume and S_{sample} is the sample surface.

This was however only the initial estimate of the coating thickness as we do not know the surface of the exact same uncoated pellet sample. Initial coating thickness estimate was followed by the iterative computational approximation procedure, where subtracting coating thickness from coated pellets semi-axis and recalculating sample surface enabled us to iteratively approach the true surface of the pellet sample before coating and thus estimate the actual coating thickness value. Thickness for each pellet time sample was calculated as an average of 3 parallel calibration samples (RSD < 5%).

Hue median was determined by scanning 8000 pellets for each time point of each calibration experiment. Thickness data were plotted against hue values to establish colorimetric calibration curve after fitting third-degree polynomial to the dataset. Due to differences in the incoming raw material Tartrazine content, two calibration curves were prepared, $t = -0.0003\times h^3 + 0.0661\times h^2 - 4.7727\times h + 117.31$ for experiments T5–T8 and $t = -0.0011371\times h^3 + 0.17253\times h^2 - 9.1433\times h + 170.98$ for experiments T1–T4 and T9–T10, where t denotes the coating thickness and h the pellet hue.

Evaluation of the Total and Residual Coating Thickness RSD and of the Preferential Coating Slope

For each experiment, > 20,000 pellets were measured for their equivalent circular diameter (ECD) and hue median.

Using the colorimetric calibration curve, coating thickness for each pellet was determined and the average coating thickness ($avg_{(t)}$) and the standard deviation (SD) of the coating thickness were calculated. Relative standard deviation (RSD) was then calculated as $RSD = SD / avg_{(t)} \times 100\%$.

A graph representing coating thickness for each pellet as a function of their size was drawn, and the linear regression was used to yield a line equation where its slope ***k*** is describing the strength of the preferential coating of a coating experiment. Slope value describes the distinctness of the particle coating thickness depending on the size of the pellets and was derived for the individual coating equipment and selected settings of coating parameters.

For the obtained coating thicknesses, the total RSD was calculated, and based on scattering around the value of the previously fitted line, the variation of the residual RSD was calculated using the next equation:

$$RSD_{res} = \frac{100\%}{\sqrt{N-1}} \times \sqrt{\sum_i^N \left(\frac{(t_i - I(t_i)}{I(t_i)} \right)^2}$$

where t_i represents colorimetrically determined coating thickness of individual pellet, N is the number of evaluated pellets, and the $I(t_i)$ denotes the coating thickness as estimated from the preferential coating line equation.

RSD_{res} describes the variation in coating thickness, which is not caused by preferential coating, but emerges because of interparticle shading phenomenon influencing the per-particle variability of amount of coating received in each pass through the spraying area and because of the variability of particle circulation times. The number of particle traversals through the spraying area during the entire coating time on the other hand reduces effects of both variations.

Statistical Treatment of Data—Preferential Coating Slopes

The linear regression was used on individual particle size and coating thickness datasets to yield a line with slope k. Independent sample t test was used to compare slopes of regression lines for equality. Samples were significantly different if $p < 0.05$.

Evaluation of Prolonged-Release Pellets' Specific Surface per Units of Volume and Mass

Prolonged-release pellet size and coating thickness were optically measured using the same two-step approach used for Tartrazin-coated pellets. Test was performed for pellet size fractions of 800–900 µm, 900–1000 µm, and 1000–1120 µm, where the key parameter was pellet size. Knowing the exact mass of the sample (m (pellet); ~ 2 g), number of particles (N), and semi-axis parameters (a, b) for each particle, we were able to calculate their volume V_1 and calculate specific surfaces per mass SSA_m and volume SSA_v using the following equations:

$$V_1 = \frac{4}{3}\pi ab^2$$

$$SSA_V = \frac{\overline{S}_1}{\overline{V}_1}$$

$$SSA_m = \frac{\overline{S}_1 \times N}{m(\text{pellet})}$$

Coating Process Yield Evaluation

Coating process yield (γ) was calculated by using the following equation:

$$\gamma = \frac{m_f \times (1 - LOD_f) - m_s \times (1 - LOD_s)}{m_{susp} \times \omega}$$

where m_f and m_s are final and starting masses of pellets in the coater, m_{susp} is the mass of sprayed coating suspension, ω is the amount of dry matter in the suspension, and LOD_f and LOD_s are the final and starting pellet loss on drying (LOD) values.

Loss on Drying

Loss on drying (LOD) was determined by placing sample of pellets (~ 5 g) on a balance equipped with halogen light heat source (HX204, Mettler Toledo, USA) and heating the sample while recording exact sample relative mass loss for 20 min at 85 ºC.

Product Separation by Sieving

Pellet separation by vibrational sieving was performed by placing 100 g of prolonged-release pellet sample on a sieve tower consisted of sieves with nominal sizes of 800 µm, 900 µm, 1000 µm, and 1120 µm and exposed to vibrations for 10 min using vibrating sieve shaker Retsch AS200 (Retsch, Germany). A 100-µm difference was large enough to separate the whole pellet distribution width into smaller distributions which could have different release profiles.

Assay and Dissolution Testing

Prolonged-release coated pellet (PR) size fractions (800–900 µm, 900–1000 µm, and 1000–1120 µm) were tested for drug assay and dissolution profile. Content of drug in final PR-coated pellets was determined on 2 parallels, where

approximately 300 mg of coated pellets was used in each parallel. Sample was placed in a 100-mL volumetric flask, and 70 mL of medium (prepared by mixing 100 mL 0.1 M NaOH (aq) with methanol and diluted to 1000 mL mark with the same solvent) was added. After pellets disintegrated using ultrasonic bath for approximately 15 min, sample was diluted with medium to 100 mL. Ten milliliter of obtained drug solution was centrifuged (4000 rpm), and 3.0 mL of clear solution was diluted to 200 mL. UV–visible spectrophotometry was used to determine sample model drug concentration at wavelength of 281 nm.

Dissolution testing with pH change approach was used to determine the release kinetics of model drug from pellets and to analyze resulting dissolution profiles in terms of their similarity with the goal of verifying comparability of individual film-coated pellet batches. Dissolution testing was performed using approximately 260 mg of coated pellets per sample, which corresponds to 100 mg of drug, while each dissolution test consisted of 3 parallels. The rotating basket dissolution method was used during testing (100 rpm, basket height 25 ± 2 mm, temperature of 37°C). Initial dissolution medium for the first 2 h consisted of 750 mL 0.1 M HCl with pH 1.2 (first dissolution sample was taken after 2 h); then after 2 h, second dissolution medium was established by adding 250 mL of 0.2 M $Na_3PO_4 \cdot 12H_2O$ to raise pH to 6.8. Dissolution samples were then taken after 3, 4, 5, and 6 h. UV–vis spectrophotometry was used to determine sample model drug concentration at wavelength of 281 nm.

To numerically evaluate similarity of release profiles, we calculated similarity f_2 factors using the following equation:

$$f_2 = 50 \times \log\left(\frac{1}{\sqrt{1 + \frac{1}{n} \times \sum_{t=1}^{n}(R_t - T_t)^2}} \times 100\right)$$

where n is number of time points, R_t is % of drug released for profile 1 in time point t, and T_t is % of released drug for profile 2 in time point t.

Two drug release profiles are deemed similar when f_2 is above 50 [23].

Results and Discussion

Results of Tartrazin Dye Coating Experiments

Results of coating process yield, average coating thickness, coating thickness RSD_{tot}, RSD_{res}, and preferential coating line slope for film-coating experiments using Tartrazine dye are represented in Table II.

Residual RSD Values of Coating Thickness

Residual RSD values evaluate the width of the coating thickness distribution independent of pellet size. A comparison of all experiments (Table II) shows a comparable range of scatter of the coating thickness regardless of the scale used (RSD_{res} between 7.7% and 9.6%). In case of GPCG1 coater, where CW distribution plate was interchanged with the funnel-shaped SW_B type of distribution plate, the use of swirl generator demonstrated a reduction of RSD_{res}, especially at the lower the gap size. However, in case of BX FBD10 equipment, interchange of CW and flat SW_A distribution plates did not alter RSD_{res} values if values are compared for the same gap size. RSD_{res} values were in this specific case surprisingly low for the CW implementation of the distribution plate. This can be most probably attributed to the fact that coating experiments T5 and T6 exhibit roughly double coating times (t_{coat}) in comparison with experiments T1 and T2 and according to Mann renewal theory the RSD of coating thickness diminishes with $1/\sqrt{t_{coat}}$ [24, 25]. The

Table II Process Conditions and Coating Results for Coating Experiments Using Tartrazine Dye

Exp	Load (kg)	DP	Gap (mm)	Spraying time (min)	Air flow (m^3/h)	LOD (%)	Yield (%)	Coating thickness (μm)	RSD_{tot} (%)	RSD_{res} (%)	Line slope (k) ($\times 10^3$)
T1	1	CW	10	106	130	1.20	79.5	11.80	12.2	9.6	+12.9
T2	1	CW	20	103	130	1.13	81.4	12.20	10.2	9.2	+7.7
T3	1	SW_B	10	107	130	1.19	79.1	11.87	7.7	7.7	−0.1
T4	1	SW_B	20	108	130	1.25	82.6	12.47	9.0	9.0	+0.2
T5	3	CW	25	201	145	1.01	93.1	15.28	8.9	8.1	+8.9
T6	3	CW	15	233	145	0.86	89.2	15.46	9.0	8.0	+10.3
T7	3	SW_A	25	201	145	1.01	92.5	15.17	8.7	8.2	+7.4
T8	3	SW_A	15	210	145	0.93	82.8	14.93	8.5	8.0	+7.5
T9	15	SW_A	10	308	450	0.75	87.9	14.73	9.9	8.4	−12.2
T10	15	SW_A	20	305	450	0.83	94.4	15.70	8.6	7.9	−8.4

pilot-scale coater (BX FBD30) demonstrated values that are directly comparable to results obtained for both FBD coaters at the lab scale. Such results can be ascribed to the equipment scale-up approach, where the number of inner tubes is increased instead of their diameter. Low overall RSD_{res} values when using SW plates can be attributed to a diminished effect of interparticle shading of the pellets in the spray zone, since the swirl air flow distributes the pellets more evenly throughout the volume of the inner tube [18].

Evaluation of Size-Based Preferential Coating of Pellets

The total and the residual RSD of the coating thickness are different, if differently sized pellets exhibit size preferential coating (if there is no preferential coating, they are the same, as in experiments T3 and T4). The degree of size preferential coating is evaluated by the slope (k value) of the linear dependence of the coating thickness and pellet size. When the k value is positive, larger particles receive more coating and vice versa, when it is negative, smaller pellets receive more coating.

Effect of Equipment Size and Distribution Plate Design on Preferential Coating

Laboratory Scale The results clearly show the difference between the individual equipment, since in the case of the GPCG laboratory coater (experiments from T1 to T4, Table II and Fig. 1a), the slope is positive when using a classic distribution plate (CW); however in the case of using swirl flow (SW), there is little or no slope [21]. On bigger laboratory scale (BX FBD10), the slope is positive for both distribution plate design; however again, a greater preferential coating is seen in the case of a classic distribution plate (Fig. 1b).

It was surprising to find out that swirl generator (SW) equipped coaters GPCG1 and BX FBD10 did not exhibit comparable size preferential coating result. While in case of experiments T7 and T8 with SW plate, a significant reduction has been observed in the slope value of size preferential coating in comparison with T5 and T6 experiments conducted in BX FBD10 with a CW plate ($p \leq 10^{-5}$ for both T5 *vs*. T7 and T6 *vs*. T8); a much greater reduction in slope (flat line) has been observed in case of SW experiments on GPCG1 (T3 and T4) in comparison with analogue counterpart experiments T1 and T2 conducted with CW plate. Observed difference in coater performance could be attributed to the fact that in case of GPCG1, a funnel-shaped SW distribution plate has been used, while in case of BX FBD10, a flat one was used (Fig. 2). Funnel-shaped distribution plate could have aid to the reduction of size preferential coating due to diminished effect of dead zone due to inclined plate surface at the outer perimeter near coater wall [17, 19], which could diminish segregation effect. It is assumed that SW distribution plate reduces size preferential coating by pushing vertical pellet flow away from the nozzle tip [18] and by imposing a more radially oriented trajectory of pellets after moving past the top edge of the draft tube and thus equilibrating the trajectories for large and small pellets. The latter effect has been presumably diminished in case of BX FBD10 as higher air flow rate has been used and inverted shape configuration of filters has been used in comparison with GPCG1, thus allowing higher maximum particle trajectories with lesser equilibration of trajectories of differently sized pellets.

Pilot Scale In the case of pilot-scale coater where the distribution plate with three swirl flow generators was used, the size preferential coating slope is negative for both experiments, indicating a preferential coating of smaller particles. Preferential coating of smaller particles has not yet been observed in the studies carried out so far and is thus exclusively related to coating in this coater modification. The understanding of the phenomenon is facilitated by Fig. 3, which represents a pilot-scale coating experiment using the same SW distribution plate, where pellet size distribution has been followed by means of two in-line dynamic image analysis systems (PATVIS APA, Sensum d.o.o., Slovenia) [26]. The image analysis system at the upper position assessed pellet size distribution in the particle fountain region, while the lower one at the coater wall of the pellet bed region. Results depicted in Fig. 3 demonstrate that the outer portion of the pellet bed is consistently richer in larger particles in comparison with the pellet size distribution in the pellet fountain region. This indicates horizontal segregation in the bed region, where smaller particles "land" closer to the cylinder and, as a result, enter subsequent coating cycle faster and consequently more often within total coating time than larger pellets. Due to greater distance between the chamber wall and the coating tube in larger coaters, the influence of any horizontal segregation of particles of different sizes can be a reason for a size preferential coating. The trajectories described by the differently sized particles in the coating cycle are to some extent defined by the presence or absence of the swirl generator, and additionally by the geometry of the coating chamber itself. Its height and the inclination of the wall can affect the height and the angle of the particle rebound from the coater wall in the pellet downward flow region and thus form the basis for the pellet size segregation in the bed region.

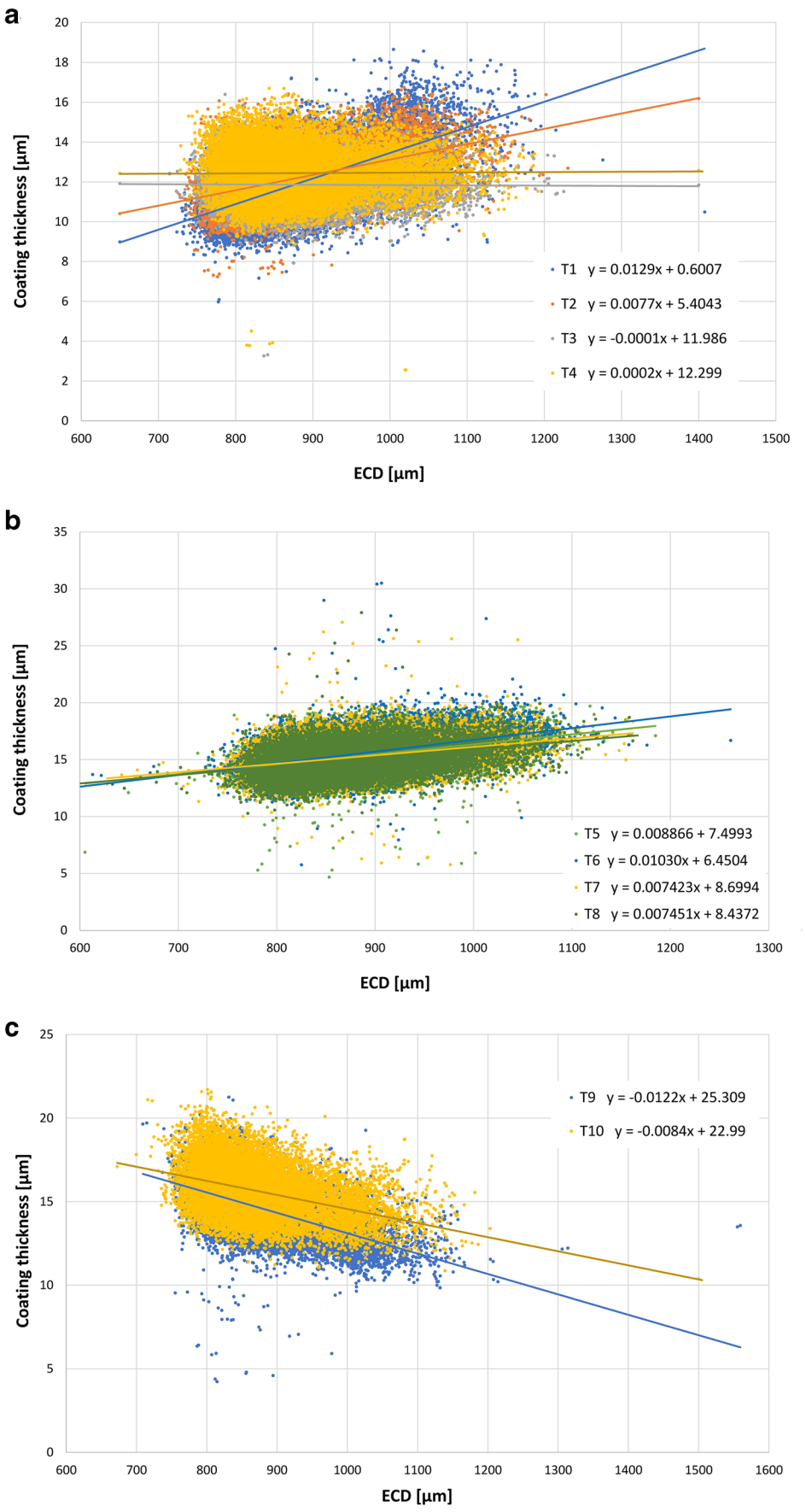

Fig. 1 Representation of size preferential coating of pellets, shown as the slope of a line showing average coating thickness as function of pellet size, presented for coating experiments: **a** T1 to T4 performed in GPCG1 coater, **b** T5 to T8 performed in BX FBD10, and **c** T9 and T10 performed in BX FBD30

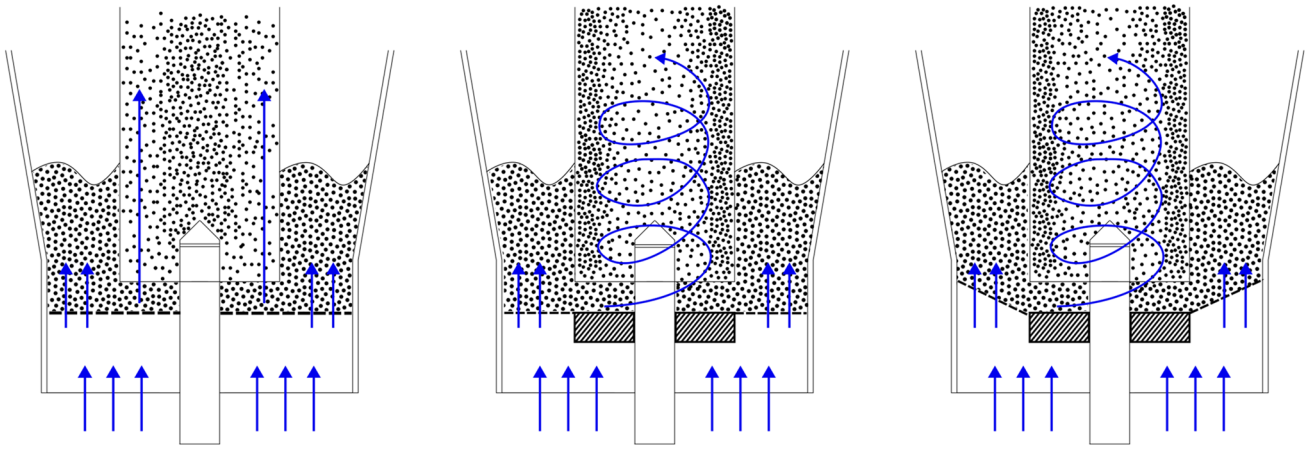

Fig. 2 Schematic representation of used distribution plates **a** classic Wurster plate (CW), **b** flat distribution plate with swirl generator (SW_A), and **c** funnel-shaped distribution plate with swirl generator (SW_B)

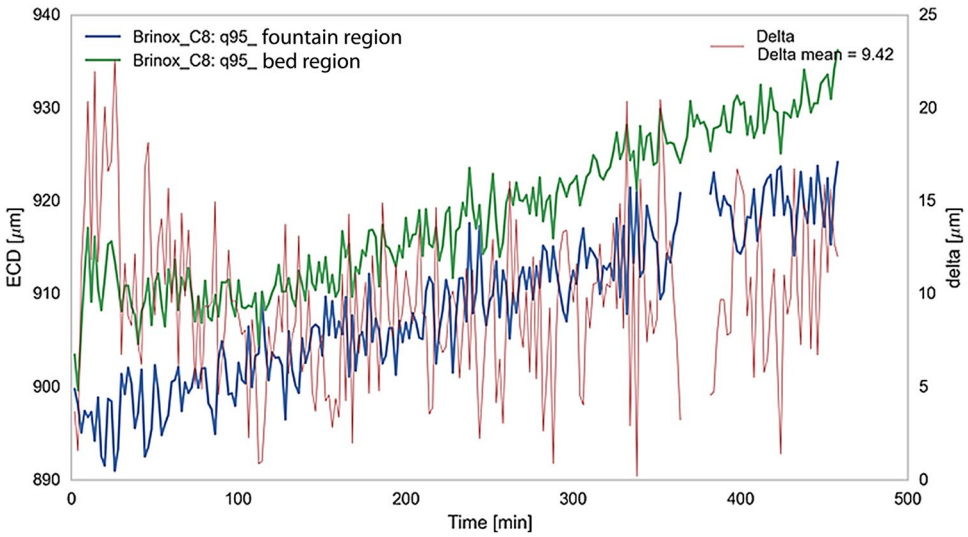

Fig. 3 Values of 95th percentiles of the pellet size distribution measured through the coating experiment by dynamic image analysis system in the pellet fountain region and in the bed region

Effect of the Gap Size Between the Distribution Plate and the Draft Tube on Preferential Coating

Laboratory Scale For coating experiments performed on GPCG1 and BX FBD10 with the CW distribution plate (T1 and T2, T5 and T6), the *k* value is significantly smaller ($p < 10^{-5}$) when using greater gap between the draft tube and the distribution plate (25 and 20 mm *vs*. 15 and 10 mm). At a lower position of the inner tube, the movement of pellets in the bed area is decreased [18] and, if segregation occurs during coating, the differences are preserved due to deficient mixing in the pellet bed region. Segregation can occur because pellets of different sizes have different accelerations inside the tube and thus expressing differences in pellet trajectory length. Larger pellets with lower ratio of drag force to mass and thus shorter trajectories will thus enter the spraying area more often and receive more coating through the overall coating time. With greater gap size, mixing in bed region is better [18], so differences in segregation are reduced. Therefore, preferential coating is less pronounced in this case. In addition, larger distance between the tube and the distribution plate at given fluidization air rate increases the mass flow of pellets through the cylinder and thus the number of circulations of pellets through the coating area [16]. Increase in circulation events together with mixing therefore reduces size preferential coating slope. When using SW distribution plate within both laboratory coaters, the difference in gap size did not have a significant effect on slope *k* value (*p* value 0.05 for experiments T3 *vs*. T4 and 0.89 for experiments T7 *vs*. T8).

Pilot Scale The previously discussed phenomenon of horizontal segregation of particles in the bed region can be reduced by more effective mixing of the particles in the bed region, namely by establishing conditions for bubbling fluidization [18]. For this purpose, pilot-scale coater (BX FBD30) was equipped with draft tubes having pressure taps at the inner bottom and upper part of the tube, thus enabling in-line measurement of pressure drop (ΔP) along the draft tube length. Pressure drop dynamics correlates with pellet vertical transport perturbations, which are when using adequate fluidizing air flow rate an indication of bubbling fluidization and thus of mixing of the particles in the accompanying bed region [27]. The pilot-scale coating experiment T10, where greater gap was used, had higher SD of ΔP (1.548 mbar) and exhibited significantly lower-size preferential coating slope value (−0.0084) than experiment T9 with slope value of −0.0122 and SD of ΔP (0.317 mbar) where smaller gap was used ($p < 10^{-5}$). This finding is consistent with the proposal that mixing in the bed region can reduce size preferential coating, as a consequence of reduction of local pellet size-based segregation.

Results of Prolonged-Release Coating Experiments

Drug-layered pellets were film-coated using a pilot-scale fluid-bed coater (BX FBD30) and a lab-scale coater (BX FBD10). Experiments at pilot scale (PR1 and PR2) were conducted with the aim of maintaining high and low fluctuations of pressure drop along the inner tubes and hence influencing the size preferential coating slope as demonstrated in experiments with Tartrazine dye. Experiments at the lab scale were corrected for the air flow to diminish the height of the particle trajectories and hence presumably reduce the variation in number of coating cycles for large and small pellets as a consequence of a difference in particle trajectory length. Coating conditions, LOD values, and yields for prolonged-release (PR) film-coating experiments are represented in Table III.

After the thermal curing process, the drug-containing pellets with PR coating were sifted and their mass proportions within individual size classes (800–900 µm, 900–1000 µm, and 1000–1120 µm) were determined. Pellet size distribution results show that the size distribution did not change in its span and its basic shape is comparable for all prolonged-release coating experiments (Table IV). The volume distribution of the pellet size is not symmetrical, as the smallest pellet size fraction (800–900 µm) dominates. Based on the data on the number of pellets per unit of mass (N/m) for individual mass fractions given in Table IV, we can calculate that the largest number of pellets in the unsieved pellet samples belongs to the size fraction of 800–900 µm (approximately 59% of the total in number), while the larger fractions are on average numerically roughly equally represented (~20% in number). Based on our previous research [14, 28], we are assuming that due to the greater representation of the pellet fraction from 800 to 900 µm in the pellet stream in terms of its surface, particle number, and due to interparticle shadowing, these will during coating process receive more coating and therefore the previously assessed native particle size-dependent preferential coating mode of coaters may be slightly changed in the outcome. It can be assumed that with the higher amount of coating, received by the smaller particle size fraction, this will diminish the effect of higher specific surface per unit of mass and contribute to equalization of drug release profiles of different coated pellet size fractions.

Results of Dissolution Testing

In order to show the difference in the release of particles of different sizes, we performed dissolution tests for the extreme pellet fraction, i.e., 800–900 µm and 1000–1120 µm. The absolute difference in % of the released active substance, where percent drug released from larger pellets size fraction is subtracted from the analogous value of the smaller pellet size fraction for each sampling time point, is presented in Table V. A positive value means that the release from larger pellets was faster, and a negative one implicates faster release from smaller pellets.

Table III Process Conditions and Coating Results for Prolonged-Release Coating Experiments

Exp	Load (kg)	DP	Gap (mm)	Spraying time (min)	Nozzle (mm)	Air pressure (bar)	Avg. airflow (m^3/h)	Air humidity (g/kg)	LOD (%)	Yield (%)
PR1	10	SW_A	20	83	3×1.2	2.2	550	3	1.09	NA*
PR2	10	SW_A	10	84	3×1.2	2.2	550	3	1.01	66.2
PR3	4	CW	25	133	1×1.2	2.0	115	1	1.08	83.5
PR4	4	SW	25	116	1×1.2	2.0	121	1	0.86	84.1
PR5	4	SW	15	112	1×1.2	2.0	123	1	1.07	66.3

*Exact mass consumption of the coating dispersion was not verifiable

Table IV Size Evaluation for PR Pellets

Exp	Sieve analysis		*a* (μm)	*b* (μm)	*m* (mg)	N/m (1/mg)	SSAm ($\mu m^2/mg \times 10^6$)
	Nominal size fraction (μm)	(% w/w)					
Drug-coated pellets	**800–900**	46.2	470.5	451.7	2000.5	2.016	5.366
	900–1000	28.0	508.0	481.76	2001.0	1.463	4.459
	1000–1120	25.4	548.4	529.2	2000.2	1.045	3.772
PR1	**800–900**	49.2	471.5	453.93	2000.3	1.831	4.891
	900–1000	23.3	502.3	478.1	2000.5	1.502	4.550
	1000–1120	26.5	550.3	529.2	2000.5	1.107	4.027
PR2	**800–900**	49.3	476.3	455.1	2000.7	1.780	4.816
	900–1000	21.7	518.6	497.4	2001.2	1.358	4.352
	1000–1120	28.8	550.3	529.2	2001.5	1.073	3.896
PR3	**800–900**	50.5	476.3	455.1	2000.6	1.823	4.943
	900–1000	22.4	516.4	494.2	2001.2	1.422	4.510
	1000–1120	26.7	550.3	529.7	2001.2	1.126	4.109
PR4	**800–900**	48.3	476.3	455.1	2000.2	1.823	4.928
	900–1000	22.6	506.7	486.4	2000.8	1.543	4.749
	1000–1120	28.6	549.9	529.2	2000.0	1.128	4.089
PR5	**800–900**	50.0	476.3	455.1	2000.6	1.756	4.735
	900–1000	20.6	508.0	486.8	2000.4	1.418	4.415
	1000–1120	29.3	549.0	529.2	2000.7	1.103	3.987

Table V Absolute Difference in % Released Active Substance and f_2 Factor Between the Largest and Smallest Fraction: Data not Normalized to the Particle Surface Area

	PR1	PR2	PR3	PR4	PR5
3 h	+3.9%	+16.5%	−8.6%	−3.9%	−6.4%
4 h	+4.5%	+13.7%	−3.4%	−4.8%	−5.6%
5 h	+3.2%	+9.4%	−8.1%	−4.5%	−6.0%
6 h	+4.9%	+6.1%	−9.0%	−6.2%	−4.5%
f_2	70	47	58	67	63

Pilot Scale In pilot-scale experiment PR1, we managed to achieve comparable drug profiles for both size fractions (f_2 factor for extreme fractions was 70, Fig. 4a), which means that configuration used canceled out the influence of SSA_m of differently sized pellets. Such outcome is highly desirable as it gives robust drug dissolution profile even if coated pellets potentially segregate before or during capsule filling. In experiment PR2, the preferential coating of larger particles was expressed to the extent that the release profile was much faster for largest pellets, which means that substantially less coating was applied to them (f_2 factor for extreme fractions was 47, Fig. 4b). Larger pellets have in the first place a slower release profile with a coating of the same thickness already due to the smaller SSA_m. These observations are additionally confirmed by the derived release profiles, which were normalized to the surface of the pellets (Supplementary material, Fig. S1).

The results of PR1 and PR2 confirm the results of the first part of this study, where it was found that the coater BX FBD30 clearly preferentially coats smaller particles to a greater extent, if the pressure drop variation along the inner tube is lower. For the given experiments PR1 and PR2, with the same filling and fluidization air flow, we set the gap to achieve larger pressure fluctuations in experiment PR1 (gap 20 mm, $\Delta P = 7–10$ mbar) than in experiment PR2 (gap 10 mm, $\Delta P = 2.5–3$ mbar). Smaller fluctuations of the pressure drop in the inner cylinder are, as already previously proposed, associated with less efficient mixing of pellets in the pellet bed area of the coater. This enables the expression of preferential coating of pellets of different sizes depending on the different trajectories of the particles and hence on the horizontal segregation of differently sized particles as demonstrated in the Tartrazine pilot-scale coating experiments. According to the dissolution results, the right level of preferential coating of smaller pellets was achieved in the case of the coating experiment PR1. Theoretically, the right level of the preferential coating should compensate for difference in SSA_m of different-sized particles and should adhere to the coating process outcome with ratio of $d_L / d_S = t_S / t_L$, where d_L and t_L denotes the diameter and PR coating thickness of larger pellets and d_S and t_S the diameter and PR coating thickness of smaller pellets.

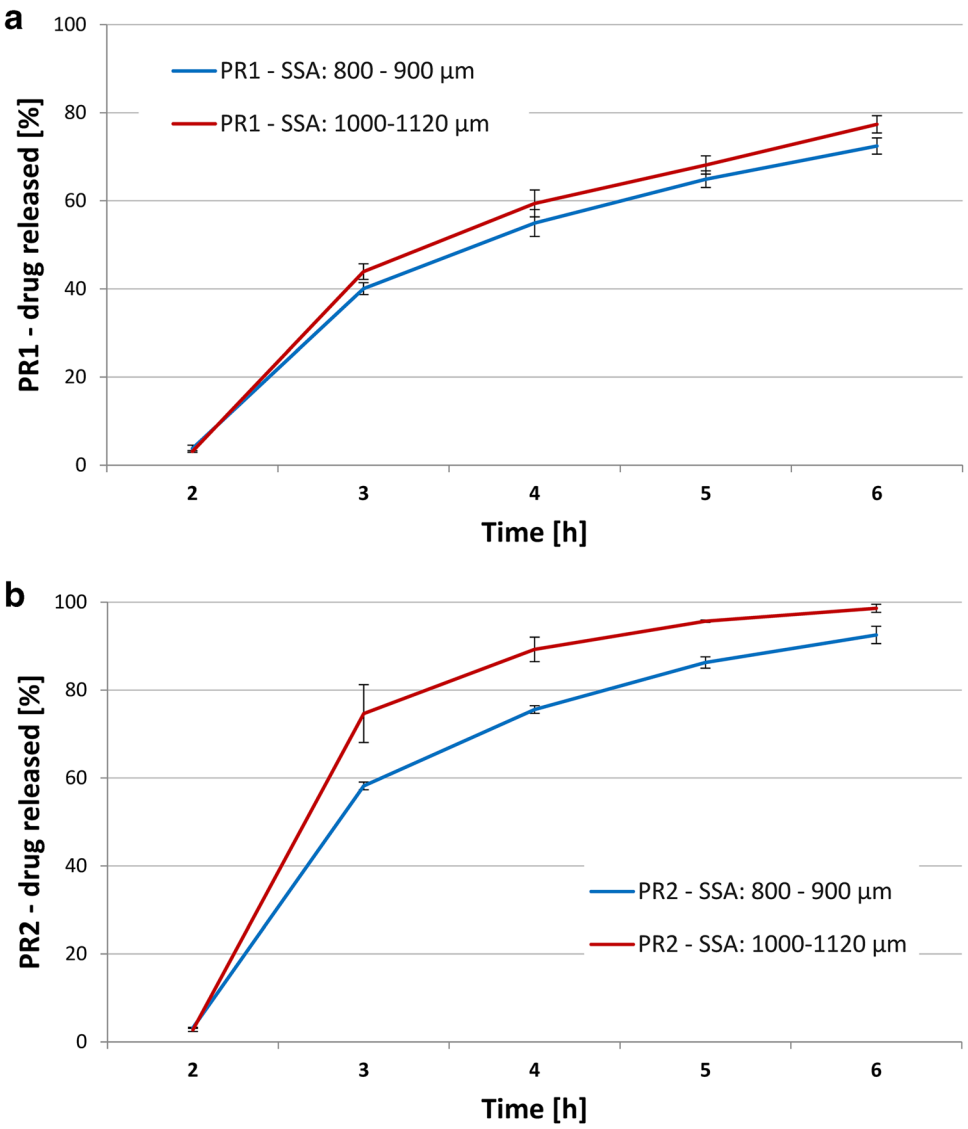

Fig. 4 Dissolution profile of pellet fractions 800–900 µm and 1000–1120 µm for pilot-scale experiments: **a** PR1 and **b** PR2

Laboratory Scale In experiments PR3 to PR5, the effects of SW and CW distribution plates and the effect of gap size within the SW distribution plate were investigated for the fluid-bed coater at the laboratory level (BX FBD10). The differences in the obtained drug release profiles are minor; they are slightly larger only in PR3 coating experiment, which was performed with a CW distribution plate. In this experiment, drug release is fastest from the smallest pellet fraction (800–900 µm), followed by the intermediate fraction (900–1000 µm) and then the largest pellets (1000–1120 µm); f_2 factor for extreme fractions is however still above 50, i.e., 59 (Fig. 5a). For the CW distribution plate, it was expected (based on literature reports and on Tartrazine experiments T5 to T8) that larger pellets would receive more coating and hence exhibit even slower drug release profile in comparison to the smaller pellet size fraction. If drug release profiles are normalized to pellet surface area per unit mass SSA_m (Supplementary material, Fig. S2a), it is demonstrated that the applied coating thickness is relatively independent of pellet size, proving that the differences in non-normalized drug dissolution data are rather the consequence of different SSA_m and not the size preferential pellet coating phenomenon.

The unexpected result obtained with Wurster's classical distribution plate could potentially be the result of the bimodal size distribution of the drug-coated pellets used in PR film-coating experiments in comparison to unimodal Cellets 700 size distribution used in Tartrazin coating experiment (Fig. 6). The analysis of pellet number portion in individual size fractions of drug-coated pellets indicates that most particles are of the smallest fraction, which in particle flow during coating obtain a larger portion of applied coating. This effect may have obscured the otherwise size preferential

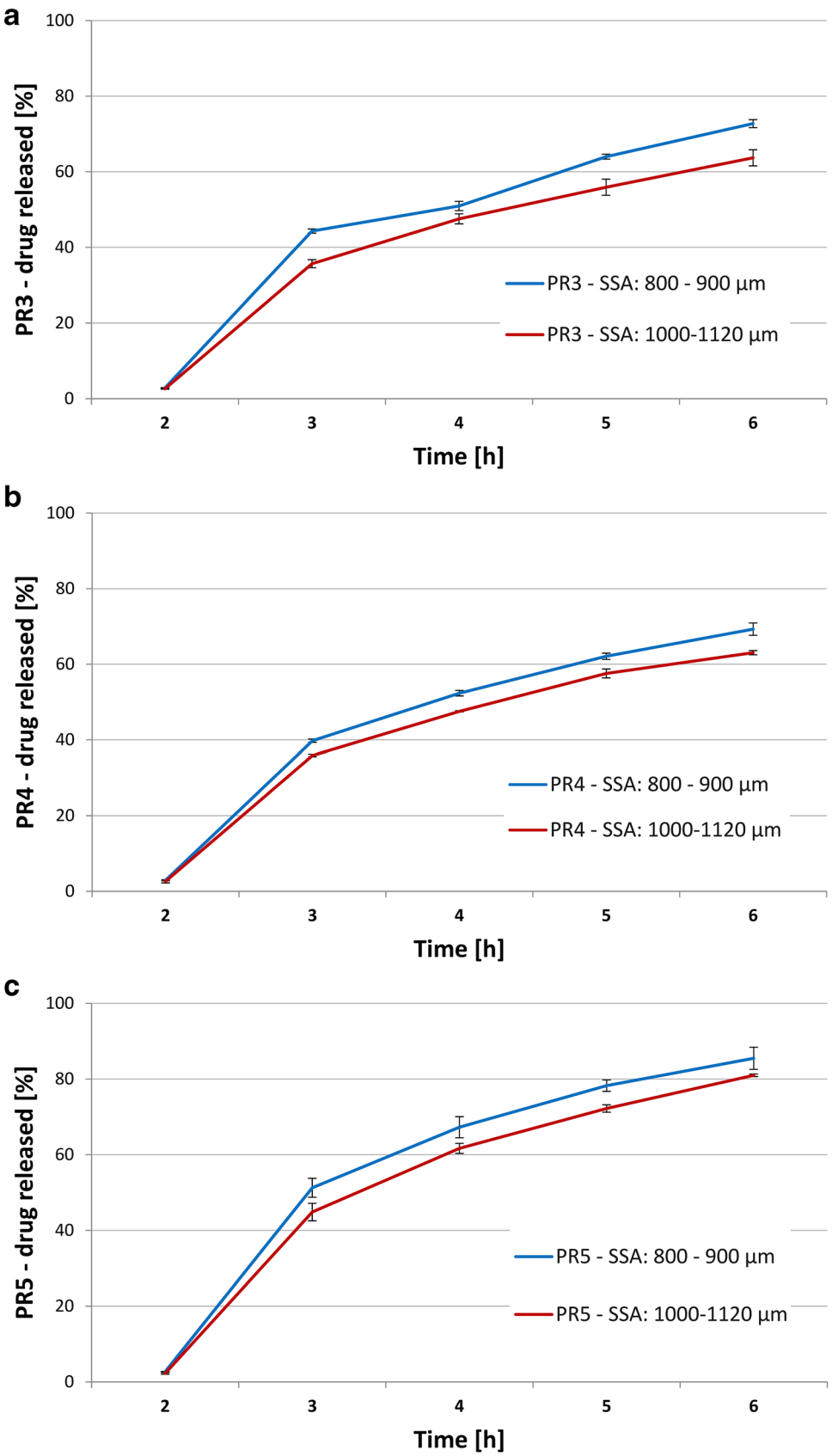

Fig. 5 Drug dissolution profiles of pellet size fractions 800–900 µm and 1000–1120 µm for laboratory-scale experiments: **a** PR3, **b** PR4, and **c** PR5

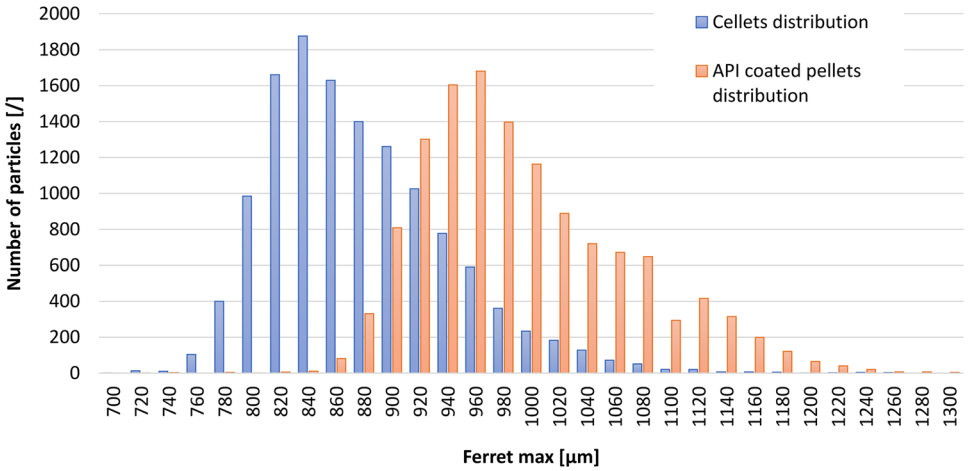

Fig. 6 Size distributions of uncoated Cellets 700 used in Tartrazine coating experiments and of drug-layered pellets used in PR coating experiments

coating profile with the positive slope, which is otherwise typical for the CW type of process chamber. Additionally, as the coating process was corrected for lower air flow in case of PR coating experiments, differences in trajectory lengths of differently sized pellets may have been reduced. Moreover, time series of size preferential slopes from the calibration experiment with Tartrazine reveals that the slope value evolves and increases with coating time, and the coating experiment PR3 is roughly two-thirds in duration in comparison with the coating experiment T5 (133 min *vs*. 201 min).

In experiments PR4 and PR5 performed using a swirl flow generator (SW), we managed to obtain comparable non-normalized drug dissolution profiles (Fig. 5b, c) between the extreme size fractions of pellets ($f_2 = 67$ for PR4 and $f_2 = 63$ for PR5). Its SSA_m normalized profiles show even higher normalized profile of a larger pellet size fraction, indicating a smaller coating thickness for bigger pellets (Supplementary material, Fig. S2b and S2c). When comparing normalized profiles of PR4 and PR5 coating experiments, we even proved a negative slope of the size preferential coating. However, the analysis of the coating processes with Tartrazine (experiments T5 to T8) did not confirm that, as in both cases slightly positive slopes of the preferential coating profiles were obtained. The discrepancy between the two results can be explained by the previous interpretation that the asymmetric bimodal numerical distribution of drug-layered pellets favors the smaller pellets during coating, which in turn obscures the native characteristic of the coater. The number-based size distribution of the input Cellets starting pellets was more uniform in the case of coating with Tartrazine dye. Additionally, also in the case of PR4 and PR5 experiments, lower inlet air flow and shorter coating times were used in comparison with coating experiments with Tartrazine (experiments T7 and T8).

The difference in drug dissolution profiles between coating experiments PR4 and PR5, where gap sizes of 20 mm and 15 mm were used, respectively, is negligible (Fig. 5b, c). This finding is in line with size preferential coating slopes of experiments T7 and T8.

Based on the obtained overall drug dissolution results, we can conclude that there are differences between the distribution plates used at the laboratory scale (BX FBD10); however, they are relatively small. As deducted from SSA_m normalized drug dissolution profiles, the coating thickness was similar for pellets of different sizes in case of both distribution plate types, which is usually desirable in the coating process. However, when coating with an PR coating, it turns out that coating with a SW distribution plate is more suitable, because in case of the experiment PR3 with a CW plate, we obtained greater differences between the non-normalized drug release profiles of different size fractions of pellets (Fig. 5a) compared to the release profiles obtained with SW distribution plate (PR4 and PR5, Fig. 5b, c).

Coating Process Yields on a Laboratory Scale

Regardless of the distribution plate type, used on a laboratory scale (BX FBD10), the yield of coating experiments was always higher when bigger gap between distribution plate and inner tube was used during coating (Tables II and III). Namely, the gap limits the entry of particles into the spraying area and determines their number density inside the cylinder during coating [28]. The higher the density of the particles, the more likely it is that droplets of the coating dispersion will effectively reach them and form a coating. There will therefore be fewer losses due to the effect of spray drying, in which the droplets dry too quickly and are eliminated from the process or applied to the inner surface of the draft tube [29].

At the same gap, we also compared the efficiency depending on the type of distribution plate used. With a larger, more optimal gap, the efficiency between the two distribution plates of the same coater is comparable (experiments T5 and T7 and experiments PR3 and PR4).

In larger laboratory experiments, smaller gap size leads to noticeable difference in process yield—the yield is quite higher using classical plate (89.2% *vs*. 82.8% for experiments T6 and T8). The reason is that SW enables better drying due to the helical path of the particle [20, 30]. The particles thus reside inside the inner cylinder for a longer time, where the local air flow is the greatest, and additionally due to the conditions of tangential air movement, the pneumatic pull of the pellets through the gap is somewhat weaker at the same global air volume flow rate, which makes the flow of pellets less dense. The unwanted effect of spray drying is thus more pronounced, so more coating liquid is lost during the coating process [28, 29].

Conclusion

Considering the results of the coating process evaluation with the dye-coated pellet approach, based on previous research, it can be said that the obtained positive slopes of size preferential coating in the laboratory-scale CW process chamber are within the expected performance of this type of coater design. The values of the slope of the size preferential coating were always lower in the case of the SW distribution plate in comparison with the CW design of the distribution plate. However, within the laboratory-scale coater designs, different performances of swirl generator equipped flat and funnel-shaped distribution plates were identified, the latter exhibiting the least size dependent preferential coating performance. This was attributed to a less expressed dead zone effect enabling mixing and elimination of any segregation in the pellet bed region of the coater. On the pilot film-coating scale, coater equipped with flat SW distribution plates exhibited negative size preferential coating slope, meaning that smaller pellets obtained more coating than larger ones, which is unprecedented result. Moreover, the extent of the negative size preferential coating slope depended on the dynamics of the pressure drop fluctuations. This finding was effectively translated to the prolonged-release coating application, where the right extent of the negative size preferential coating ensures pellet size-independent drug release profiles, thus improving robustness of such multiple unit prolonged-release formulation. By lowering the air flow rate and using bimodal size distribution, rich in smaller drug-layered pellets, led to rather surprising results, where performance of prolonged drug release-coated pellets did not resemble size preferential coating results from the dye coating study part.

These results confirm the fact that we must have a good knowledge of the coater performance characteristics in combination with the process variables and even formulation properties, if we want to produce coated multiple-unit solid pharmaceutical products of the highest quality.

Supplementary Information The online version contains supplementary material available at https://doi.org/10.1208/s12249-023-02540-9.

Acknowledgements The authors would like to thank KRKA d.d., Novo mesto, and Brinox d.o.o. for support in equipment and material supplied for this study. Authors acknowledge Domen Kitak from Sensum d.o.o. for support in in-line measuring of particle size distributions.

Author Contribution Conceptualization, T.B., G.H., M.L., and R.D.; methodology, T.B., G.H., M.P., and R.D.; formal analysis, T.B., G.H., and R.D.; investigation, T.B., M.L., and M.P.; resources, T.B. and R.D.; writing—original draft preparation, T.B.; writing—review and editing, G.H., M.L, M.P., and R.D.; visualization, T.B. and R.D.; and supervision, R.D. All authors have read and agreed to the published version of the manuscript.

Funding This research was funded by the Slovenian Research Agency under grant numbers P1-0189 and P2-0162. The APC was funded by the Faculty of Pharmacy, University of Ljubljana.

Data Availability The datasets generated during and/or analysed during the current study are not publicly available due to collaboration with Krka d.d., Novo mesto, Brinox d.o.o. and Sensum d.o.o., which supported study with equipment and materials. Public data sharing beyond data included in this published article (and its supplementary information files) was not envisaged and negotiated at the beginning of the study. Data are available from the corresponding author on reasonable request and with permissions of Krka d.d., Novo mesto, Brinox d.o.o. and Sensum d.o.o.

Declarations

Conflict of Interest The authors declare no competing interests.

References

1. Wagner KG, Krumme M, Schmidt PC. Investigation of the pellet-distribution in single tablets via image analysis. Eur J Pharm Biopharm. 1999;47(1):79–85.
2. Chopra R, Alderborn G, Podczeck F, Newton JM. The influence of pellet shape and surface properties on the drug release from uncoated and coated pellets. Int J Pharm. 2002;239(1–2):171–8.
3. Ghebre-Selassie I. Pharmaceutical Pelletization Technology. Taylor & Francis; 1989. 296 p.
4. Cole G, Aulton ME, Hogan JE, editors. Pharmaceutical coating technology. London ; Bristol PA: Taylor & Francis; 1995. 489 p.
5. Ahmed I, Roni MA, Kibria G, Islam MR, Jalil R ul. In vitro Release kinetics study of ambroxol hydrochloride pellets developed by extrusion spheronization technique followed by acrylic polymer coating. Dhaka Univ J Pharm Sci. 2008;7(1):75–81.

6. Sudsakorn K, Turton R. Nonuniformity of particle coating on a size distribution of particles in a fluidized bed coater. Powder Technol. 2000;110(1–2):37–43.
7. Hampel N, Bück A, Peglow M, Tsotsas E. Continuous pellet coating in a Wurster fluidized bed process. Chem Eng Sci. 2013;86:87–98.
8. Dreu R, Srčič S, Luštrik M. Primerjava in razvoj naprav za oblaganje delcev. Farm Vestn. 2010;3(61):155–61.
9. Christensen FN, Bertelsen P. Qualitative description of the wurster-based fluid-bed coating process. Drug Dev Ind Pharm. 1997;23(5):451–63.
10. Wesdyk R, YMJ. The effect of size and mass on the film thickness of beads coated in fluidized bed equipment. Int J Pharm. 1990;65(1–2):69–76.
11. Cheng XX, Turton R. The prediction of variability occurring in fluidized bed coating equipment. II. The role of nonuniform particle coverage as particles pass through the spray Zonemr. Pharm Dev Technol. 2000 Jan;5(3):323–32.
12. Chan LW, Tang ESK, Heng PWS. Comparative study of the fluid dynamics of bottom spray fluid bed coaters. AAPS PharmSciTech. 2006;7(2):E37.
13. Marucci M, Holmgren A, Carlsson H, Jarke A, Johansson M, von Corswant C. Non-uniformity of pellets coating, effect on the dose release profile andhow to improve the coating process by reducing the electrostatic charging of the pellets. Chem Biochem Eng Q. 2012;26(4):379–84.
14. Luštrik M, Dreu R, Šibanc R, Srčič S. Comparative study of the uniformity of coating thickness of pellets coated with a conventional Wurster chamber and a swirl generator-equipped Wurster chamber. Pharm Dev Technol. 2010;17(3):268–76.
15. Cheng XX, Turton R. The prediction of variability occurring in fluidized bed coating equipment. I. The measurement of particle circulation rates in a bottom-spray fluidized bed coater. Pharm Dev Technol. 2000 Jan;5(3):311–22.
16. Kitak D, Šibanc R, Dreu R. Evaluation of pellet cycle times in a Wurster chamber using a photoluminescence method. Chem Eng Res Des. 2018Apr;132:1170–9.
17. Shelukar S, Ho J, Zega J, Roland E, Yeh N, Quiram D, et al. Identification and characterization of factors controlling tablet coating uniformity in a Wurster coating process. Powder Technol. 2000;110(1–2):29–36.
18. Luštrik M, Šibanc R, Srčič S, Perpar M, Žun I, Dreu R. Characteristics of pellet flow in a Wurster coater draft tube utilizing piezoelectric probe. Powder Technol. 2013;235:640–51.
19. Dreu R, Luštrik M, Perpar M, Zun I, Srčič S. Fluid-bed coater modifications and study of their influence on the coating process of pellets. Drug Dev Ind Pharm. 2012;38(4):501–11.
20. Heng PWS, Chan LW, Tang ESK. Use of swirling airflow to enhance coating performance of bottom spray fluid bed coaters. Int J Pharm. 2006;327(1–2):26–35.
21. Šibanc R, Luštrik M, Dreu R. Analysis of pellet coating uniformity using a computer scanner. Int J Pharm. 2017;533(2):377–82.
22. Xu D, Cui J, Bansal R, Hao X, Liu J, Chen W, et al. The ellipsoidal area ratio: an alternative anisotropy index for diffusion tensor imaging. Magn Reson Imaging. 2009;27(3):311–23.
23. Moore JW, Flanner HH. Mathematical comparison of dissolution profiles. Pharm Technol. 1996(20 (6)):64–74.
24. Mann U. Analysis of spouted-bed coating and granulation. 1. Batch operation. Ind Eng Chem Process Des Dev. 1983 Apr;22(2):288–92.
25. Turton R. Challenges in the modeling and prediction of coating of pharmaceutical dosage forms. Powder Technol. 2008;181(2):186–94.
26. Oman Kadunc N, Šibanc R, Dreu R, Likar B, Tomaževič D. Inline monitoring of pellet coating thickness growth by means of visual imaging. Int J Pharm. 2014;470(1):8–14.
27. Perpar M, Luštrik M, Dreu R, Srčič S, Žun I. Estimating coating quality parameters on the basis of pressure drop measurements in a Wurster draft tube. Powder Technol. 2013;246:41–50.
28. Šibanc R, Žun I, Dreu R. Measurement of particle concentration in a Wurster coater draft tube using light attenuation. Chem Eng Res Des. 2016;110:20–31.
29. Turk M, Šibanc R, Dreu R, Frankiewicz M, Sznitowska M. Assessment of mini-tablets coating uniformity as a function of fluid bed coater inlet conditions. Pharmaceutics. 2021;13(5):746.
30. Özbey M, Söylemez MS. Effect of swirling flow on fluidized bed drying of wheat grains. Energy Convers Manag. 2005;46(9–10):1495–512.